# Higgs bosons with large transverse momentum at the LHC ☆

Kirill Kudashkin [b], Jonas M. Lindert [a], Kirill Melnikov [b], Christopher Wever [b,c]

[a] *Institute for Particle Physics Phenomenology, Durham University, Durham, DH1 3LE, UK*
[b] *Institute for Theoretical Particle Physics (TTP), KIT, Karlsruhe, Germany*
[c] *Institut für Kernphysik (IKP), KIT, 76344 Eggenstein-Leopoldshafen, Germany*

## ARTICLE INFO

## ABSTRACT

We compute the next-to-leading order QCD corrections to the production of Higgs bosons with large transverse momentum $p_\perp \gg 2m_t$ at the LHC. To accomplish this, we combine the two-loop amplitudes for processes $gg \to Hg$, $qg \to Hq$ and $q\bar{q} \to Hg$, recently computed in the approximation of nearly massless top quarks, with the numerical calculation of the squared one-loop amplitudes for $gg \to Hgg$, $qg \to Hqg$ and $q\bar{q} \to Hgg$ processes. The latter computation is performed with OpenLoops. We find that the QCD corrections to the Higgs transverse momentum distribution at very high $p_\perp$ are large but quite similar to the QCD corrections obtained for point-like $Hgg$ coupling. Our result removes one of the largest sources of theoretical uncertainty in the description of high-$p_\perp$ Higgs boson production and opens a way to use the high-$p_\perp$ region to search for physics beyond the Standard Model.

## 1. Introduction

Detailed exploration of the Higgs boson is one of the central tasks of the particle physics program at the LHC. Since the majority of the Higgs bosons is produced in the gluon fusion, it is only natural to study Higgs coupling to gluons as precisely as possible.

Incidentally, the Higgs–gluon coupling is very interesting phenomenologically. Indeed, since the Higgs coupling to gluons is loop-induced, and since contributions of heavy particles whose masses are generated by the Higgs mechanism do not decouple, the $ggH$ interaction vertex becomes an intriguing probe of the TeV-scale physics.

In the Standard Model, the $ggH$ interaction vertex is almost entirely generated by the top quark loops and, since the top Yukawa coupling in the Standard Model is fully determined by the top quark mass, it appears that the $ggH$ coupling is fully predictable. However, since the top Yukawa coupling is known experimentally to about 50 percent from $ttH$ production process [1,2], it is still possible that there is additional, point-like component of the $Hgg$ coupling that appears thanks to physics beyond the Standard Model (BSM).

To describe this possibility, we consider the following modification of the top Yukawa part of the SM Lagrangian

$$\frac{m_t}{v}\bar{t}tH \to -\kappa_g \frac{\alpha_s}{12\pi}\frac{1}{v}G_{\mu\nu}^a G^{\mu\nu,a}H + \kappa_t \frac{m_t}{v}\bar{t}tH. \tag{1}$$

The first term on the r.h.s. in Eq. (1) is the point-like contribution to the Higgs–gluon coupling and the second is the modified top Yukawa coupling.

What are the constraints on the anomalous couplings $\kappa_g$ and $\kappa_t$ from the Higgs production in gluon fusion? Since the top quark contribution to Higgs boson production in gluon fusion is well-described in the large-$m_t$ approximation, the production cross section is proportional to the sum of the two couplings squared $\sigma_{gg \to H} \sim \alpha_s^2/v^2(\kappa_g + \kappa_t)^2$. Clearly, even if the cross section $\sigma_{gg \to H}$ is measured with absolute precision, we cannot constrain $\kappa_g$ and $\kappa_t$ separately but only their sum.

To disentangle $\kappa_g$ and $\kappa_t$, one has to go beyond total cross section measurements. A useful and simple observable [3] is the Higgs boson transverse momentum distribution. Indeed, if we assume that scale of New Physics[1] that generates point-like $ggH$ coupling proportional to $\kappa_g$, is much larger than twice the top quark mass, there exists a range of transverse momenta $2m_t \ll p_\perp \ll \Lambda_g$ such that the BSM contribution to the Higgs–gluon vertex can still be treated as point-like, whereas the top quark contribution starts

[1] We refer to such a scale as $\Lambda_g$.

being resolved. This feature can be illustrated by the following schematic formula

$$\frac{d\sigma_H}{dp_\perp^2} \sim \frac{\sigma_0}{p_\perp^2} \begin{cases} (\kappa_g + \kappa_t)^2, & p_\perp^2 < 4m_t^2, \\ \left(\kappa_g + \kappa_t \frac{4m_t^2}{p_\perp^2}\right)^2, & p_\perp^2 > 4m_t^2. \end{cases} \qquad (2)$$

This formula suggests that a measurement of the Higgs transverse momentum distribution in the two regions, $p_\perp \ll 2m_t$ and $p_\perp \gg 2m_t$, allows for a separate determination of $\kappa_g$ and $\kappa_t$.

There are quite a few obstacles to a practical realization of this program. First, assuming that $\kappa_t \sim 1$, $\kappa_g \sim 0.1$, the $p_\perp$ distribution of the Higgs boson is dominated by the Standard Model contribution until rather high values of the Higgs transverse momentum. Unfortunately, since the cross section decreases quite fast with $p_\perp$, we expect a relatively small number of events in the interesting transverse momentum region. For example, the SM cross section for producing Higgs bosons with transverse momenta larger than 450 GeV is close to $\mathcal{O}(10 \text{ fb})$; therefore, even allowing for small deviations from the Standard Model, we estimate that just a few hundred Higgs bosons have been produced in the high-$p_\perp$ region at the LHC so far.

Second, even if Higgs bosons with high transverse momenta are produced, identifying them through standard clean decay channels $H \rightarrow \gamma\gamma$ and $H \rightarrow 4$ leptons decreases the number of events because of the tiny branching fractions of these decay modes. In fact, the number of events is reduced to such an extent that, given current integrated luminosity, it becomes impossible to observe them.

The third point concerns the quality of the theoretical description of the Higgs $p_\perp$ spectrum at high transverse momentum. As follows from Eq. (2), we require the description of the spectrum in two regimes: a) $p_\perp < 2m_t$, where the $ggH$ interaction is, effectively, point-like and b) $p_\perp > 2m_t$ where, in addition to the point-like interaction, there is a "resolved", $p_\perp$-dependent component due to the top quark loop. Theoretical description of Higgs boson production in gluon fusion, for a point-like gluon–Higgs vertex, is extremely advanced. Indeed, the inclusive rate for gluon fusion Higgs production in this approximation is known to the astounding $N^3LO$ QCD accuracy [4], and the Higgs $p_\perp$-distribution has been computed to NNLO QCD [5–7].

In comparison, very little is known about gluon fusion *beyond* the point-like approximation for the $ggH$ interaction vertex which becomes of particular relevance at high $p_\perp$. The corresponding cross section was computed at leading order in perturbative QCD [8] *thirty years ago* and only recently this result was extended to next-to-leading order in a situation when the mass of the quark that facilitates the Higgs–gluon interaction is much smaller than the Higgs boson mass and all other kinematic invariants in the problem [9,10].

We emphasize that even if the first and second points that we mentioned earlier can be overcome, imprecise knowledge of the Standard Model contribution at high $p_\perp$ may be an obstacle for the determination of $\kappa_g$. Indeed, since the two contributions to $d\sigma/dp_\perp^2$ at high $p_\perp$ may receive different radiative corrections, lack of their knowledge may affect the interpretation of the result especially if relatively small values of $\kappa_g$ are to be probed. Since for processes with gluons in the initial state large QCD corrections are typical, one can expect large radiative corrections also for the resolved top-quark loop at high $p_\perp$. Although the fact that radiative corrections are large is almost guaranteed, the important question is by how much they differ if the high-$p_\perp$ tail of the Higgs transverse momentum distribution is computed with the point-like or "resolved" Higgs–gluon vertex. This is the question that we attempt to answer in this paper.

It is clear that the low statistics issue, that was mentioned in the first and second points above, can only be overcome by collecting higher integrated luminosity; luckily, the LHC will continue doing that. However, it should be possible, already now, to perform relevant measurements in the high-$p_\perp$ region if one does not lose so much statistics by insisting that the produced Higgs bosons should decay into clean final states. Interestingly, it appears to be possible to do that. Indeed, in contrast to low-$p_\perp$ Higgs production, at high-$p_\perp$ one can identify the Higgs boson through its decays to $H \rightarrow b\bar{b}$ using the boosted techniques [11] and to distinguish hadronically-decaying Higgs bosons from large QCD backgrounds. In fact, the CMS collaboration has recently presented results of the very first analysis [12] performed along these lines, where Higgs boson production with $p_\perp > 450$ GeV, was observed. Although the result for the Higgs production cross section with $p_\perp > 450$ GeV obtained in [12] is rather imprecise, forthcoming improvements with higher luminosity and better analysis technique are to be expected.

The third point mentioned above is an important issue. Indeed, since the Standard Model production of a Higgs boson at high $p_\perp$ involves "resolved" top quark loops, computing next-to-leading order QCD corrections to this process requires dealing with two-loop four-point functions with internal (top quark) and external (Higgs boson) massive particles. The relevant two-loop Feynman integrals with the full dependence on $m_t$ and $m_H$ are still not available,[2] so that the NLO QCD computation can not be performed. Thus, in the literature various approximations have been performed both for inclusive Higgs production [13] and also for finite Higgs $p_\perp$ [14,15]. However, recently, the two-loop amplitudes for the production of the Higgs boson at high-$p_\perp$ were computed [16]. This result enables calculation of the Higgs boson transverse momentum distribution for $p_\perp > 2m_t$ at NLO QCD, that we report in this Letter.

The rest of the paper is organized as follows. In the next Section, we provide a short summary of theoretical methods used for the calculation of two-loop virtual and real emission corrections. Phenomenological results are reported in Section 3. We conclude in Section 4.

## 2. Computational setup

We begin with the discussion of the computation of the two-loop QCD amplitudes for producing the Higgs boson with large transverse momentum in proton collisions [16]. There are four partonic processes that contribute; they are $gg \rightarrow Hg$, $g\bar{q} \rightarrow H\bar{q}$, $gq \rightarrow Hq$ and $q\bar{q} \rightarrow Hg$. We systematically neglect the Higgs boson coupling to light quarks; therefore, all contributions to scattering amplitudes are mediated by the top quark loops and are proportional to the top quark Yukawa coupling.

In principle, scattering amplitudes for Higgs boson production with non-vanishing transverse momentum depend on the Higgs boson mass, the top quark mass and two Mandelstam invariants $s$ and $t$. Computation of two-loop Feynman integrals that depend on such a large number of parameters and, moreover, contain internal massive lines, is, currently not feasible. However, since we are interested in describing production of the Higgs boson with *high* transverse momentum, we can construct an expansion of the scattering amplitude in $m_i^2/s$ and $m_i^2/p_\perp^2$, where $m_i^2 \in \{m_H^2, m_t^2\}$. Additionally, as $m_H^2/(2m_t)^2 \sim 0.1$, it is motivated to neglect the Higgs boson mass compared to the top quark mass in the computation.

It is however non-trivial to construct such an expansion in the Higgs and top quark masses. Indeed, in contrast to an opposite

---

[2] We note that planar two-loop integrals for this process were computed in Ref. [17].
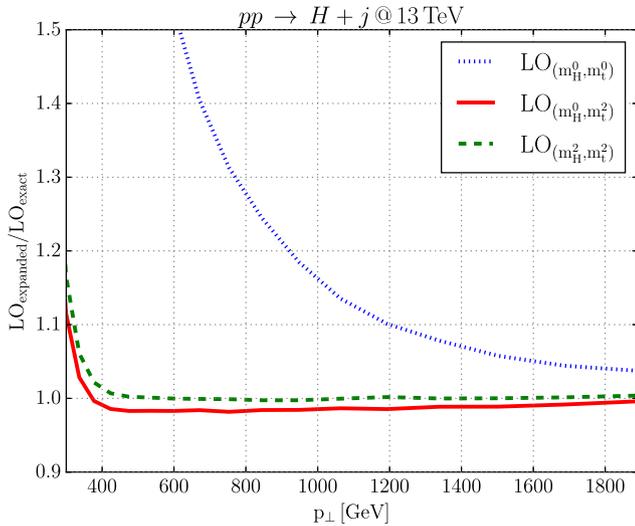
**Fig. 1.** Ratio of approximate to exact leading order cross sections. By retaining $\mathcal{O}(m_t^2/p_\perp^2)$ corrections in scattering amplitudes (red line), we obtain an excellent approximation to the exact LO result. The notation $m_t^0$ and $m_t^2$ in the legend of the plot refers to the leading and next-to-leading power expansion of the amplitude in $m_t^2$, not including the overall $m_t^2$ that arises from the Yukawa coupling and the helicity flip. (For interpretation of the colors in the figure(s), the reader is referred to the web version of this article.)

kinematic limit, $p_\perp \ll m_t$, where expansion of scattering amplitudes can be performed at the level of Feynman integrals in momentum space using the large-mass expansion algorithms [18], no momentum-space algorithms exist for an expansion in the small quark mass. For this reason, we have opted for a different method [19,9]. The idea is to first derive differential equations for master integrals[3] that are *exact* in all kinematic parameters and then develop a systematic expansion of these differential equations in the mass of the top quark and the Higgs boson. Since the differential equations contain all the information about the possible singularities of the solutions, we can construct the expansion of the solutions in the limit of small Higgs and top masses.

We have applied this method to compute all the master integrals relevant for the Higgs+jet production amplitudes [16]. When computing these amplitudes, we have retained first sub-leading terms in the $m_t^2/p_t^2$-expansion but we have set the mass of the Higgs boson to zero.[4] It turned out that by keeping sub-leading terms in the $m_t^2/p_\perp^2$-expansion in the amplitude we can significantly extend the applicability range of the computation. To illustrate this, in Fig. 1, we compare the exact leading order $p_\perp$ distribution of the Higgs boson with three expansions. We see that the result for amplitude expanded to $\mathcal{O}(m_H^0, m_t^2)$ terms tracks the leading order amplitude at the level of few percent all the way down to the top quark threshold; on the contrary, if the subleading top quark mass terms are not retained, the expanded and exact cross sections have $\mathcal{O}(20\%)$ difference at $p_\perp \sim 800$ GeV. Even higher terms in the $m_t^2/p_\perp^2$-expansion do not further improve the agreement at the scale of Fig. 1. Yet, keeping also subleading terms in the $m_H^2$ expansion can further improve the agreement with the exact result. For illustration, in Fig. 1 we show the result for the amplitude expanded up to $\mathcal{O}(m_H^2, m_t^2)$, which above threshold agrees at the permil level with the exact result. Including even

higher expansions does not yield further improvement visible at the scale of Fig. 1.

In order to produce physical results for Higgs boson production with non-vanishing transverse momentum, we need to combine the above discussed virtual corrections with the corresponding real corrections, e.g. $gg \to H + gg$, $qg \to Hq + g$ etc, that describe inelastic processes. Computation of one-loop scattering amplitudes for these inelastic processes is non-trivial; it requires evaluation of five-point Feynman integrals with massive internal particles. Nevertheless, these amplitudes are known analytically since quite some time [20].[5]

In this Letter we follow an approach, based on the automated numerical computation of one-loop scattering amplitudes developed in recent years. One such approach, known as Open-Loops [21], employs a hybrid tree-loop recursion. Its implementation in the OpenLoops program is publicly available [22,23]. This program has been applied to compute one-loop QCD and electroweak corrections to a multitude of complicated multi-leg scattering processes (see e.g. Refs. [24,25]) and for the real-virtual contributions in NNLO computations (see e.g. Ref. [26]).

For these applications in NNLO calculations and for computing NLO corrections to loop-induced processes, such as the one discussed here, the corresponding one-loop real contributions need to be computed in kinematic regions where one of the external partons becomes soft or collinear to other partons. A reliable evaluation of the one-loop scattering amplitudes in such kinematic regions is non-trivial, but OpenLoops appears to be perfectly capable of dealing with this challenge thanks to the numerical stability of the employed algorithms. A major element of this stability originates from the employed tensor integral reduction library COLLIER [27].

All virtual and real amplitudes have been implemented in the POWHEG-BOX [28], where infra-red singularities are regularized using FKS subtraction [29]. All OpenLoops amplitudes are accessible via a process-independent interface developed in Ref. [25]. The implementation within the POWHEG-BOX will allow for an easy matching of the fixed-order results presented here with parton showers at NLO.

## 3. Results

In this Section, we present the results of our computation of the NLO QCD corrections to Higgs boson production at high $p_\perp$. We consider proton–proton collisions at the LHC with the center of mass energy 13 TeV. The Higgs boson mass[6] and the top quark mass[7] are taken to be $m_H = 125$ GeV and $m_t = 173.2$ GeV, respectively. We employ the five-flavor scheme and consider the bottom quark as massless parton in the proton. We use the NNPDF3.0 set of parton distribution functions [30] at the respective perturbative order and employ the strong coupling constant $\alpha_s$ that is provided with these PDF sets. We choose renormalization and factorization scales to be equal and take as the central value

$$\mu_0 = \frac{H_T}{2}, \quad H_T = \sqrt{m_H^2 + p_\perp^2} + \sum_j p_{\perp,j}, \qquad (3)$$

where the sum runs over all partons in the final state. We note that at large Higgs boson transverse momentum, the scale simplifies to $\mu_0 = H_T/2 \approx p_\perp$. Theoretical uncertainties are estimated by

---

[3] The required algebraic reduction to master integrals is highly non-trivial; for this, we have used results obtained in an earlier collaboration with L. Tancredi in Ref. [9].

[4] Setting $m_H$ to zero is possible since the dependence of all amplitudes on the Higgs boson mass is analytic.

[5] These amplitudes were recently re-evaluated in Ref. [15].

[6] Although the Higgs boson mass is ignored in the two-loop virtual amplitude, it is retained in the computation of the real emission contribution to the transverse momentum distribution.

[7] We renormalize the top quark mass in the pole scheme.

**Table 1**

Inclusive cross sections and $K$-factors for $pp \to H + \text{jet}$ at $\sqrt{S} = 13$ TeV in the SM and in the infinite top mass approximation with different lower cuts on the Higgs boson transverse momentum $p_\perp$. We estimate the theoretical uncertainty in the predicted cross section by changing renormalization and factorization scales by a factor of two around the central value in Eq. (3). We define the $K$-factors as $\sigma_{\text{NLO}}/\sigma_{\text{LO}}$. The results for $K$-factors in the Table are computed for the central value of the renormalization scale. See text for details.

| | $\text{LO}_{\text{HEFT}}$ [fb] | $\text{NLO}_{\text{HEFT}}$ [fb] | $K$ | LO [fb] | NLO [fb] | $K$ |
|---|---|---|---|---|---|---|
| $p_\perp > 400$ GeV | $33.8^{+44\%}_{-29\%}$ | $61.4^{+20\%}_{-19\%}$ | 1.82 | $12.4^{+44\%}_{-29\%}$ | $23.6^{+24\%}_{-21\%}$ | 1.90 |
| $p_\perp > 450$ GeV | $22.0^{+45\%}_{-29\%}$ | $39.9^{+20\%}_{-19\%}$ | 1.81 | $6.75^{+45\%}_{-29\%}$ | $12.9^{+24\%}_{-21\%}$ | 1.91 |
| $p_\perp > 500$ GeV | $14.7^{+44\%}_{-28\%}$ | $26.7^{+20\%}_{-19\%}$ | 1.81 | $3.80^{+45\%}_{-29\%}$ | $7.28^{+24\%}_{-21\%}$ | 1.91 |
| $p_\perp > 1000$ GeV | $0.628^{+46\%}_{-30\%}$ | $1.14^{+21\%}_{-19\%}$ | 1.81 | $0.0417^{+47\%}_{-30\%}$ | $0.0797^{+24\%}_{-21\%}$ | 1.91 |

varying the renormalization and factorization scales $\mu$ by a factor of two around the central value. Finally, we note that we use both the leading order and the real-emission amplitudes for Higgs boson production with non-vanishing transverse momentum keeping full dependence on the top quark and Higgs boson masses and we only use the expansion in the top quark mass and the Higgs boson mass in the finite remainder of the two-loop amplitude.

The results of the computation are presented in Table 1 where we show the inclusive cross sections at LO and NLO together with the corresponding NLO/LO correction factors for different values of the lower cut on the Higgs transverse momentum. The inclusive cross sections are computed for both the point-like Higgs–gluon coupling, obtained by integrating out the top quark, and for the physical Higgs–gluon coupling with a proper dependence on $m_t$. We will refer to the two cases as HEFT and SM, respectively. Although the differences between HEFT and SM production cross sections grow dramatically with the increase of the $p_\perp$-cut, the radiative corrections change both cross sections by a similar amount. Indeed, the ratio of $K$-factors[8] for the $p_\perp = 400$ GeV cut and the central scale $\mu_0$ is $K_{\text{SM}}/K_{\text{HEFT}} = 1.04$ and the ratio of $K$-factors for the $p_\perp = 1000$ GeV cut is $K_{\text{SM}}/K_{\text{HEFT}} = 1.06$. Note that the $K$-factor themselves are close to 1.9, almost independent of the $p_\perp$-cut. Uncertainties due to scale variations are reduced from about 40% at LO to the level of 20% at NLO, both for a point-like Higgs–gluon coupling and in the full SM. These uncertainties are insensitive to the $p_\perp$-cut.

Finally, the Higgs boson transverse momentum distribution for $p_\perp > 300$ GeV is shown in Fig. 2. The results shown there confirm what is already seen in Table 1 – both the SM and the HEFT $K$-factors are flat over the entire range of $p_\perp$. For the central scale $\mu = \mu_0$ Eq. (3) the differences between the two $K$-factors is about five percent. The scale dependence of HEFT and SM results are also similar. The residual theoretical uncertainty related to perturbative QCD computations remains at the level of twenty percent, as estimated from the scale variation. Such an uncertainty is typical for NLO QCD theoretical description of many observables related to Higgs boson production in gluon fusion.

Another source of uncertainties is related to the choice of the renormalization-scheme of the top mass. Since the amplitude is proportional to the squared top mass, the differential cross section scales as the fourth power $d\sigma \sim m_t^4$, if we neglect suppressed terms in $m_t^2/p_\perp^2$ and the logarithms of $m_t^2/p_\perp^2$. At LO in perturbation theory, a different choice of the top-mass scheme corresponds to changing numerically the input value of the top mass. If we choose instead the $\overline{\text{MS}}$ top mass value[9] of $m_t^{\overline{\text{MS}}}(p_\perp \approx 400 \text{ GeV}) \approx 157$ GeV, we would find a decrease of the LO cross section by about $d\sigma_{\text{LO}}^{\overline{\text{MS}}}/d\sigma_{\text{LO}}^{\text{pole}} \sim (157/173)^4 \sim 0.68$. At NLO one needs to ad-
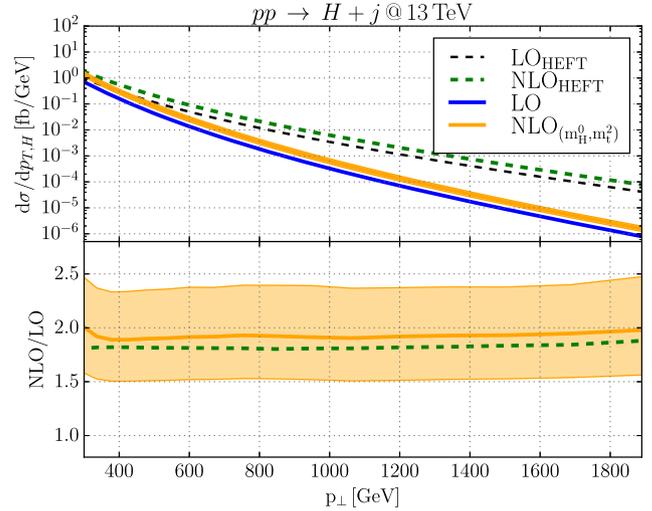


**Fig. 2.** Transverse momentum distribution of the Higgs boson at the LHC with $\sqrt{s} = 13$ TeV. The upper panel shows absolute predictions at LO and NLO in the full SM and in the infinite top-mass approximation (HEFT). The lower panel shows respective NLO/LO correction factors. The bands indicate theoretical errors of the full SM result due to scale variation.

ditionally take into account the $\alpha_s$ corrections that relate the on-shell and $\overline{\text{MS}}$ top mass values. These corrections will compensate the numerical change caused by changing $m_t = m_t^{\overline{\text{MS}}}$ to $m_t = m_t^{\text{pole}}$ in the NLO amplitudes and as a result the scheme dependence at NLO is reduced. Thus, we expect the scheme dependence at NLO to be subleading with respect to the scale uncertainties.

Further improvements in theory predictions are only possible if the proximity of the HEFT and SM $K$-factors is taken seriously and postulated to occur even at higher orders. In this case, one will have to re-weight the existing HEFT $H + j$ computations [5–7] with the exact leading order cross section for producing the Higgs boson with high $p_\perp$. In fact, such a reweighting can now be also performed at the NLO level.

## 4. Conclusions

We presented the NLO QCD corrections to the Higgs boson transverse momentum distribution at very large $p_\perp$ values. To compute them, we employed the recent calculation of the two-loop scattering amplitudes for all relevant partonic channels [16] where an expansion in $m_t/p_\perp$ was performed. The real emission corrections were computed with the Openloops [21] program. We have found that the QCD corrections to the Higgs boson transverse momentum distribution increase the leading order result by almost a factor of two. However, their magnitude appears to be quite similar to the QCD corrections computed in the approximation of a point-like Higgs–gluon vertex; the difference of the two result is close to five percent. Our computation removes the

---

[8] The $K$-factors are defined as $d\sigma_{\text{NLO}}/d\sigma_{\text{LO}}$.

[9] We calculated this value using the program RunDec [31] with the input value $m_t^{\overline{\text{MS}}}(m_t^{\overline{\text{MS}}}) = 166$ GeV.

major theoretical uncertainty in the description of the Higgs boson transverse momentum distribution at high $p_\perp$ and opens a way to a refined analysis of the sensitivity of this observable to BSM contributions using existing [12] and forthcoming experimental measurements.

## Acknowledgements

## References

[1] G. Aad, et al., ATLAS Collaboration, J. High Energy Phys. 1605 (2016) 160.
[2] M. Aaboud, et al., ATLAS Collaboration, arXiv:1712.08895 [hep-ex].
[3] C. Arnesen, I.Z. Rothstein, J. Zupan, Phys. Rev. Lett. 103 (2009) 151801.
[4] C. Anastasiou, C. Duhr, F. Dulat, E. Furlan, T. Gehrmann, F. Herzog, A. Lazopoulos, B. Mistlberger, J. High Energy Phys. 05 (2016) 058.
[5] R. Boughezal, F. Caola, K. Melnikov, F. Petriello, M. Schulze, Phys. Rev. Lett. 115 (8) (2015) 082003.
[6] R. Boughezal, C. Focke, W. Giele, X. Liu, F. Petriello, Phys. Lett. B 748 (2015) 5.
[7] X. Chen, T. Gehrmann, E.W.N. Glover, M. Jaquier, Phys. Lett. B 740 (2015) 147.
[8] R.K. Ellis, I. Hinchliffe, M. Soldate, J.J. van der Bij, Nucl. Phys. B 297 (1988) 221–243.
[9] K. Melnikov, L. Tancredi, C. Wever, J. High Energy Phys. 1611 (2016) 104.
[10] J.M. Lindert, K. Melnikov, L. Tancredi, C. Wever, Phys. Rev. Lett. 118 (25) (2017) 252002.
[11] J.M. Butterworth, A.R. Davison, M. Rubin, G.P. Salam, Phys. Rev. Lett. 100 (2008) 242001.
[12] C. Collaboration, CMS Collaboration, Inclusive search for the standard model Higgs boson produced in pp collisions at $\sqrt{s} = 13$ TeV using H$\to$ b$\bar{\text{b}}$ decays, CMS-PAS-HIG-17-026.
[13] R.V. Harlander, K.J. Ozeren, J. High Energy Phys. 0911 (2009) 088;
C. Anastasiou, S. Beerli, S. Bucherer, A. Daleo, Z. Kunszt, J. High Energy Phys. 0701 (2007) 082;
R.V. Harlander, K.J. Ozeren, J. High Energy Phys. 0911 (2009) 088;
A. Pak, M. Rogal, M. Steinhauser, J. High Energy Phys. 1002 (2010) 025;
R.V. Harlander, K.J. Ozeren, Phys. Lett. B 679 (2009) 467;
A. Pak, M. Rogal, M. Steinhauser, Phys. Lett. B 679 (2009) 473;
S. Marzani, R.D. Ball, V. Del Duca, S. Forte, A. Vicini, Nucl. Phys. B, Proc. Suppl. 186 (2009) 98;
S. Marzani, R.D. Ball, V. Del Duca, S. Forte, A. Vicini, Nucl. Phys. B 800 (2008) 127;
R.V. Harlander, H. Mantler, S. Marzani, K.J. Ozeren, Eur. Phys. J. C 66 (2010) 359.
[14] R.V. Harlander, T. Neumann, K.J. Ozeren, M. Wiesemann, J. High Energy Phys. 1208 (2012) 139;
T. Neumann, M. Wiesemann, J. High Energy Phys. 1411 (2014) 150;
E. Braaten, H. Zhang, J.W. Zhang, J. High Energy Phys. 1711 (2017) 127.
[15] T. Neumann, C. Williams, Phys. Rev. D 95 (1) (2017) 014004.
[16] K. Kudashkin, K. Melnikov, C. Wever, J. High Energy Phys. (2018), https://doi.org/10.1007/JHEP02(2018)135, submitted for publication, arXiv:1712.06549.
[17] R. Bonciani, V. Del Duca, H. Frellesvig, J.M. Henn, F. Moriello, V.A. Smirnov, J. High Energy Phys. 1612 (2016) 096.
[18] An introduction to the large-mass expansion of Feynman diagrams can be found in V.A. Smirnov, Analytic Tools for Feynman Integrals, Springer Tracts Mod. Phys., vol. 250, 2012, p. 1.
[19] R. Mueller, D.G. Öztürk, J. High Energy Phys. 1608 (2016) 055.
[20] V. Del Duca, W. Kilgore, C. Oleari, C. Schmidt, D. Zeppenfeld, Phys. Rev. Lett. 87 (2001) 122001;
V. Del Duca, W. Kilgore, C. Oleari, C. Schmidt, D. Zeppenfeld, Nucl. Phys. B 616 (2001) 367.
[21] F. Cascioli, P. Maierhöfer, S. Pozzorini, Phys. Rev. Lett. 108 (2012) 111601.
[22] The OpenLoops one-loop generator by F. Cascioli, J. Lindert, P. Maierhöfer, S. Pozzorini, publicly available at http://openloops.hepforge.org.
[23] F. Buccioni, J.M. Lindert, P. Maierhöfer, S. Pozzorini, M. Zoller, in preparation.
[24] S. Kallweit, J.M. Lindert, P. Maierhöfer, S. Pozzorini, M. Schönherr, J. High Energy Phys. 1604 (2016) 021;
S. Höche, P. Maierhöfer, N. Moretti, S. Pozzorini, F. Siegert, arXiv:1607.06934 [hep-ph];
S. Kallweit, J.M. Lindert, S. Pozzorini, M. Schönherr, J. High Energy Phys. 1711 (2017) 120.
[25] T. Jezo, J.M. Lindert, P. Nason, C. Oleari, S. Pozzorini, Eur. Phys. J. C 76 (12) (2016) 691.
[26] F. Cascioli, et al., Phys. Lett. B 735 (2014) 311;
D. de Florian, M. Grazzini, C. Hanga, S. Kallweit, J.M. Lindert, P. Maierhöfer, J. Mazzitelli, D. Rathlev, J. High Energy Phys. 1609 (2016) 151;
M. Grazzini, S. Kallweit, S. Pozzorini, D. Rathlev, M. Wiesemann, J. High Energy Phys. 1608 (2016) 140;
M. Grazzini, S. Kallweit, M. Wiesemann, CERN-TH-2017-232, ZU-TH 30/17.
[27] A. Denner, S. Dittmaier, L. Hofer, Comput. Phys. Commun. 212 (2017) 220;
A. Denner, S. Dittmaier, Nucl. Phys. B 658 (2003) 175;
A. Denner, S. Dittmaier, Nucl. Phys. B 734 (2006) 62;
A. Denner, S. Dittmaier, Nucl. Phys. B 844 (2011) 199.
[28] P. Nason, J. High Energy Phys. 0411 (2004) 040;
S. Frixione, P. Nason, C. Oleari, J. High Energy Phys. 0711 (2007) 070;
S. Alioli, P. Nason, C. Oleari, E. Re, J. High Energy Phys. 1006 (2010) 043;
T. Jezo, P. Nason, J. High Energy Phys. 1512 (2015) 065.
[29] S. Frixione, Z. Kunszt, A. Signer, Nucl. Phys. B 467 (1996) 399–442.
[30] R.D. Ball, et al., NNPDF Collaboration, J. High Energy Phys. 1504 (2015) 040.
[31] K.G. Chetyrkin, J.H. Kuhn, M. Steinhauser, Comput. Phys. Commun. 133 (2000) 43.